

Directed evolution of human T-cell receptors with picomolar affinities by phage display

Yi Li¹, Ruth Moysey¹, Peter E Molloy¹, Anne-Lise Vuidepot¹, Tara Mahon¹, Emma Baston¹, Steven Dunn¹, Nathaniel Liddy¹, Jansen Jacob¹, Bent K Jakobsen¹ & Jonathan M Boulter^{1,2}

Peptides derived from almost all proteins, including disease-associated proteins, can be presented on the cell surface as peptide–human leukocyte antigen (pHLA) complexes. T cells specifically recognize pHLA with their clonally rearranged T-cell receptors (TCRs), whose natural affinities are limited to ~1–100 μM ¹. Here we describe the display of ten different human TCRs on the surface of bacteriophage, stabilized by a nonnative interchain disulfide bond². We report the directed evolution of high-affinity TCRs specific for two different pHLAs: the human T-cell lymphotropic virus type 1 (HTLV-1) tax_{11–19} peptide–HLA-A*0201 complex³ and the NY-ESO-1_{157–165} tumor-associated peptide antigen–HLA-A*0201 complex⁴, with affinities of up to 2.5 nM and 26 pM, respectively, and we demonstrate their high specificity and sensitivity for targeting of cell-surface pHLAs.

TCRs and antibodies are the only antigen-recognition molecules of the adaptive immune system that are somatically rearranged to generate hugely diverse repertoires. In contrast to TCRs, antibodies have been routinely made in soluble form for many years⁵, can be displayed and selected *in vitro*^{6,7}, and have been used for diagnostic and therapeutic targeting⁸. Display of TCRs on yeast cells has been used to select stabilized variants of the single-chain allo-reactive mouse 2C TCR⁹ and to increase its affinity by a reported ~100-fold to 9 nM¹⁰, but similar engineering of other TCRs has not been reported. The high-affinity, single-chain 2C TCR confers high peptide sensitivity and CD8 independence to transfected T cells^{11,12}, but shows significant cross-reactivity to self-peptide antigens¹³. Phage display of a single-chain mouse TCR has also been reported¹⁴, but high-affinity TCR generation was not achieved. These technologies have therefore not had the impact of monoclonal-antibody library display, and there remains a need for a robust technology that allows display and molecular evolution of TCRs.

Recently we have described a method for producing stable TCR molecules that involves introducing an interchain disulfide bond into the interface between the TCR constant domains and which is applicable to a wide range of different TCRs². Such disulfide-stabilized TCRs can be expressed in a number of different systems (N. Pumphrey et al., unpublished data) and retain the authentic structure of a

heterodimeric $\alpha\beta$ -TCR. The versatility of this approach and the unique stability of disulfide-linked TCRs led us to explore the possibility of displaying them on the surface of bacteriophage.

Phage display of TCRs was achieved by expressing them as disulfide-linked heterodimers² fused to the geneIII product on the surface of M13 phage. We confirmed expression of phage-surface TCRs by western blotting of reduced and nonreduced samples (data not shown). Where a specific pHLA was available, phage-displayed TCRs were also functionally assayed by testing for specific binding in an enzyme-linked immuno-sorbent assay (ELISA) using streptavidin-immobilized, biotin-tagged, peptide-HLA complexes and detecting bound phage using anti-geneIII protein antibodies (Table 1; TCR genes are referred to using ImMunoGeneTics (IMGT) nomenclature¹⁵).

We selected two phage-displayed TCRs for further engineering: the A6 TCR specific for the complex between HLA-A*0201 and the HTLV-1 tax_{11–19} peptide (LLFGYPVYV) (A2-tax)^{3,16}, and the 1G4 TCR specific for the complex between HLA-A*0201 and the NY-ESO-1_{157–165} peptide (SLLMWITQC) (A2-NY-ESO)⁴. The A6 TCR was selected because of its high efficiency of folding, its relatively high affinity of 1.8 μM , and because its ligand-bound structure is known³; the 1G4 TCR was selected because it is specific for a well-validated cancer marker (NY-ESO-1). After confirmation of functional wild-type TCR display by ELISA, we generated libraries for both TCRs containing degenerate complementarity-determining regions (CDRs). We selected TCR-phage through several rounds, on the basis of binding to immobilized A2-tax or A2-NY-ESO respectively. High-affinity TCRs selected from A6 TCR-phage libraries contained mutations only in the CDR3 β chains (Table 2a), but this was almost certainly due to minor technical problems with the A6 CDR3 α libraries, which were resolved for generation of the 1G4 TCR-phage library, resulting in the selection of many high-affinity variants containing CDR3 α mutations from these libraries (Table 2b). Many selected clones also contained amber stop codons, which are partially suppressed to glutamine in the TG1 host and probably modulate the level of TCR expression, implying some toxicity of the TCR to the host. However, no significant differences in *in vitro* refolding of selected TCRs was observed (data not shown), indicating that selected TCRs have similar stabilities to the wild-type TCRs.

¹Avidex Limited, 57–59 Milton Park, Abingdon, Oxon OX14 4RX, United Kingdom. ²Present address: Department of Medical Biochemistry & Immunology, Henry Wellcome Building, School of Medicine, Cardiff University, Heath Park, Cardiff CF14 4XN, United Kingdom. Correspondence should be addressed to J.M.B. (boulterjm@cardiff.ac.uk).

Table 1 Summary of TCRs successfully displayed on phage

Name	TRAV	TRAJ	TRBV	TRBJ	HLA	Peptide	Origin	ELISA
A6	12-2	24	6-5	2-7	A2	LLFGYPVYV	HTLV-1 tax	+
1G4	21	15	6-5	2-2	A2	SLLMWITQC	NY-ESO-1	+
ILAK	22	40	6-5	1-1	A2	ILAKFLHWL	hTERT	+
LC13	26-2	52	7-8	2-7	B8	FLRGRAYGL	EBV EBNA3A	+
JM22	27	15	19	2-7	A2	GILGFVFTL	Influenza MP	nd
AH1.23	12-2	13	2-5	2-5	DR4	RHVVIDKSFQSPQIT	Chlamydial hsp60	nd
MM15	12-2	34	28	2-6	A2	AAGIGILTV	Melan A	+
1A77	12-2	39	29-1	2-2	A2	AAGIGILTV	Melan A	nd
CD1d	24	18	25-1	2-7	CD1d	α -galactyl-ceramide	Lipid	+
GRb	28-2	53	4-1	2-5	B27	SRYWAIRTR	Influenza HA	nd

The various variable and junctional gene segments of the TCRs are indicated (in IMGT nomenclature¹⁵) and the HLA-peptide ligand is also shown along with confirmation of functional activity by phage ELISA binding to pHLA, where this has been performed. nd, not determined. TRAV, TCR alpha variable segment; TRAJ, TCR alpha joining segment; TRBV, TCR beta variable segment; TRBJ, TCR beta joining segment; HLA, human leukocyte antigen specificity.

The selected TCR-displaying phage clones were ranked using an inhibition phage ELISA and a number of these TCRs were made as soluble disulfide-linked TCRs² (substituting glutamine for amber codons). Results from TCR-phage binding competition assays, along with affinity and kinetic binding data of soluble TCRs binding to peptide-HLA ligands (generated by Biacore surface plasmon resonance (SPR)), are shown in **Tables 2a,b** and **Figure 1**. We found that the improved binding of high-affinity TCRs selected by phage display is caused predominantly by slower off-rates compared with their wild-type parents.

The highest-affinity A6 TCR, obtained after one round of library generation and phage selection, was A6c134, with a K_d of 2.5 nM and a half-life of binding at 25 °C of 52 min, compared with 7.0 s for A6wt (**Fig. 1**; left panel). The 1G4 TCR was subjected to an additional round of library construction and phage selection, enabling engineering of much higher affinity. This was generated by much more extensive mutation of TCR CDR loops and loop-flanking residues (see **Table 2b**), which was enabled by the large libraries that could be successfully displayed with the TCR phage display. The highest-affinity 1G4 TCR, after two rounds of library construction and phage selection, was 1G4c113, which yielded a K_d of 20 pM, and a half-life of binding at 25 °C of ~1,000 min, compared with 7.2 s for 1G4wt (**Fig. 1**; right panel). Because we observed rebinding artifacts when using high-density (>1,000 resonance units) chip surface antigen, we coated the chip surface with minimal antigen (~150 RU). At this level of antigen density, rebinding effects were not observed, that is, no changes in TCR dissociation were observed during the dissociation phase when 1 μ M of soluble, nonbiotinylated A2-peptide complexes (free antigen) was injected over the chip surface.

To confirm the accuracy of the very high-affinity measurement for 1G4c113, we applied global curve fitting¹⁷ to Biacore SPR data generated at varying TCR concentrations (see **Supplementary Fig. 1** online). This yielded a very similar global equilibrium dissociation constant (K_d) of 26.1 (± 0.5) pM ($k_{on} = 6.59 \times 10^5$ ($\pm 1.25 \times 10^4$) s⁻¹; $k_{off} = 1.72 \times 10^{-5}$ ($\pm 6.40 \times 10^{-8}$) s⁻¹) for the binding of 1G4c113 to A2-NY-ESO. Although the dissociation phases used for global fitting were measured for a relatively short time (~1 h), they were confirmed by longer time-course experiments up to 24 h (data not shown). We further performed a competition Biacore SPR binding assay¹⁸ using soluble, nonbiotinylated A2-NY-ESO protein. Although we were unable to obtain meaningful data using TCR concentrations below 1 nM, making an accurate measurement of K_I in the 20-pM range impossible, our K_I estimate of 20 pM (see **Supplementary Fig. 2**

online) confirms the order of magnitude of our affinity measurements determined by conventional direct binding methods.

To see whether the high-affinity mutations had affected TCR specificity, we tested high-affinity TCRs A6c134 and 1G4c113 for binding to broad panels of peptide-HLA complexes (see **Supplementary Table 1** online) using the highly sensitive Biacore SPR assay. This assay can detect interactions with very low affinities (K_d s ≥ 2 mM)¹⁹. No cross-reactive binding was detectable to any of the nonindex peptide-HLA complexes.

We tested the ability of A6c134 and 1G4c113 to detect varying amounts of peptide on the cell surfaces of human HLA-A*0201⁺ cell lines. To enable high-affinity TCR detection by fluorescence-activated cell scanning

(FACS), we tetramerized the high-affinity TCRs using a biotin tag linked to R-phycoerythrin-labeled streptavidin in an analogous manner to the production of major histocompatibility complex tetramers²⁰. We then stained peptide-pulsed cells and specifically detected A2-peptide complexes at pulse concentrations down to 10 nM peptide for A6c134 and 1 nM for 1G4c113 (**Fig. 2a,b**, respectively). This is comparable to the sensitivity of many T-cell clones, and is likely limited by the sensitivity of the FACS technology used to detect staining more than the affinity of the TCR reagents, as is the case for TCR tetramers with wild-type affinity²¹.

To examine cross-reactivity to a broader panel of endogenous peptides, we analyzed A6c134 and 1G4c113 tetramer binding to a nonpulsed HLA-A*0201⁺ cell line. The background control was the same cell line pulsed at high concentration with an irrelevant peptide (10 μ M influenza M1 peptide (GILGFVFTL) for A6c134 and 10 μ M HTLV-1 tax₁₁₋₁₉ (LLFGYPVYV) for 1G4c113, to which A6c134 and 1G4c113 do not exhibit any binding, respectively, by Biacore assay), to chase off endogenous peptides. Despite the difference in endogenous peptide levels, no difference in TCR binding was observed between the two cell populations for either A6c134 or 1G4c113 (**Fig. 2**). Similar cell-targeting results were obtained using three more HLA-A*0201⁺

Table 2a Summary of output from A6 TCR phage display selection

Clone no.	CDR3 β	% inh. @ 200 nM	% inh. @ 20 nM	Kd (nM)
wt	GLAGGRPEQYF	32–36	29	1,800
1	GLV P GRPEQ*F	94	53.5	106
2	GLV S A*PEQYF	93.9	55.2	nd
83	GL* A GRPEQYF	27.4	–12.7	nd
85	GLAGGR P DQ*F	14.7	1.3	nd
86	GRSA *RPEQYF	21.9	–4.1	nd
87	GLAGGR P EA*F	19.7	1.9	nd
89	GLAGGR P ED*F	67	23	420
111	GLAGGR P HP*F	Nd	58.6	1,500
125	GLAGGR P DA*F	Nd	21.2	nd
133	GL I SA*PEQYF	Nd	nd	nd
134	GL M SA*PEQYF	95.5	60	2.5

Amino acid sequences are indicated in single-letter code with * representing amber stop codons which are suppressed to glutamine in the TG1 host. % inh. indicates the percentage inhibition of the phage binding ELISA signal to a pHLA-coated surface when preincubated with the indicated concentration of soluble pHLA. K_d s were obtained using Biacore SPR with soluble versions of the selected TCRs and A2-tax immobilized by a biotin tag to a streptavidin-coated CM-5 chip surface. Mutations shown in bold type. nd, not determined.

Table 2b Summary of output from 1G4 TCR phage display selection

Clone no.	CDR2 α	CDR3 α	CDR2 β	TCR β F3	CDR3 β	% inh. @ 200 nM	% inh. @ 20 nM	k_{on} ($M^{-1} s^{-1}$)	k_{off} (s^{-1})	K_d (nM)
WT	IQSSQ	PTSGGSYIPT	GAGI	QGEVPNGYNVSRSTT	YVGN	nd	nd	4×10^4	0.128	32000
1	IQSSQ	PTSGGSYIPT	GAGT	RGEVPNGYNVSRSTI	YLGN	26	nd	nd	nd	nd
2	IQSSQ	PTSGGSYIPT	GAGT	QGEVPNGYNVSRSTT	NVGN	24	nd	nd	nd	nd
3	IQSSQ	PTSGGSYIPT	GAGT	QGEVPNGYNVSRSTT	YVGG	24	nd	nd	nd	nd
6	IQSSQ	HTSNGYFPPT	GAGT	RGEVPNGYNVSRSTI	YLGN	99	67	3.7×10^4	3.1×10^{-4}	8.4
8	IQSSQ	PMTGGTYIPT	GAGT	QGEVPNGYNVSRSTT	NVGN	96	64	nd	nd	nd
9	IQSSQ	PLYGGTYIPT	GAGT	RGEVPNGYNVSRSTI	YLGN	91	31	nd	nd	nd
10	IQSSQ	PMIGGTYIPT	GAGT	RGEVPNGYNVSRSTI	YLGN	96	59	nd	nd	nd
11	IQSSQ	PLTGGTYIPT	GAGT	RGEVPNGYNVSRSTI	YLGN	94	48	nd	nd	nd
12	IQSSQ	PLTGGSYIPT	GAGT	QGEVPNGYNVSRSTT	NVGN	79	28	nd	nd	nd
13	IQSSQ	PATGGTYIPT	GAGT	QGEVPNGYNVSRSTT	NVGN	86	32	nd	nd	nd
14	IQSSQ	PQTVPTTYIPT	GAGT	RGEVPNGYNVSRSTI	YLGN	79	nd	nd	nd	nd
15	IQSSQ	PMSGGTYIPT	GAGT	QGEVPNGYNVSRSTT	NVGN	63	nd	nd	nd	nd
33	IQSSQ	PYQSGHYMPT	GAGT	RGEVPNGYNVSRSTI	YLGN	99	96	1.04×10^4	1.90×10^{-3}	180
33A	IQSSQ	PYQSGHYMPT	GAGT	QGEVPNGYNVSRSTI	YLGN	nd	nd	7.50×10^3	1.90×10^{-3}	254
122	ISPWQ	PLLDGTYIPT	AIQT	QGEVPNGYNVSRSTI	YVGD	nd	nd	3.04×10^4	2.97×10^{-5}	0.98
120	ITPWQ	PLLDGTYIPT	AIQT	QGEVPNGYNVSRSTI	YVGD	nd	nd	5.97×10^4	1.21×10^{-5}	0.2
112	ISPWQ	PLLDGTYIPT	AIQT	RGEVPNGYNVSRSTI	YLGN	nd	nd	3.28×10^5	3.43×10^{-5}	0.1
119	ITPWQ	PLLDGTYIPT	AIQT	QGEVPNGYNVSRSTI	YVGN	nd	nd	6.50×10^4	6.59×10^{-6}	0.1
121	ISPWQ	PLLDGTYIPT	AIQT	QGEVPNGYNVSRSTI	YVGN	nd	nd	1.15×10^5	1.16×10^{-5}	0.1
107	ISPWQ	PFTGGGYIPT	AIQT	QGEVPNGYNVSRSTT	YVGN	nd	nd	4.26×10^5	1.83×10^{-5}	0.04
113	ITPWQ	PLLDGTYIPT	AIQT	RGEVPNGYNVSRSTI	YLGN	nd	nd	6.59×10^5	1.72×10^{-5}	0.026

Amino acid sequences are indicated in single-letter code. % inh. indicates the percentage inhibition of the phage-binding ELISA signal to a pHLA-coated surface when preincubated with the indicated concentration of soluble pHLA. K_d s were obtained using Biacore SPR with soluble versions of the selected TCRs and A2-NY-ESO immobilized by a biotin tag to a streptavidin-coated CM-5 chip surface. Mutations shown in bold type. nd, not determined.

cell lines (data not shown), demonstrating that neither high-affinity TCR has any detectable cross-reactivity to endogenous peptide-HLA-A*0201 complexes.

Successful *in vivo* targeting of cells with high-affinity TCRs must require high levels of specificity as the density of specific peptide-HLA on a natural cell surface is likely to be low ($\leq 1,000$ per cell²²) compared with the background of endogenous peptide-HLA. The high-affinity TCRs we have generated show extremely high levels of specificity. Indeed, recent data show that A6c134 specificity is enhanced compared with its A6wt parent²¹, presumably because high affinity is selected on the basis of positive binding to the cognate target and will therefore only increase cross-reactivity in the very small number of instances in which elements of the cross-reactive pHLA are structurally identical to the cognate target. Given the huge diversity of different endogenous peptides presented on the surface of host cells by HLA molecules, it is likely that very high-affinity and high-specificity TCRs, such as the 26 pM affinity 1G4c113 TCR, will be preferable for effective therapeutic and diagnostic targeting.

High-affinity TCRs generated by phage display have a variety of potential biomedical applications: as targeting agents in cancers to deliver either a therapeutic 'payload' of a cytotoxic material or an immune stimulatory conjugate, or as inhibitory agents to block specific autoimmune T-cell activation. They should also be valuable diagnostic reagents enabling detection and measurement of specific peptide-HLA complexes, both on the surface of cells and in intracellular processing pathways, in those diseases for which peptide antigens have been identified. Studies designed to prove the principle of high-affinity TCR targeting in a variety of diseases are currently under way.

Recently, a number of peptide-HLA-specific monoclonal antibodies have been generated²³, including some specific for A2-tax^{24,25} and A2-NY-ESO²⁶. However, their affinities are still relatively weak (~ 25 – 30 nM for the A2-tax antibody and 60 nM for the A2-NY-ESO antibody) compared with the A6c134 and 1G4c113 high-affinity TCRs described here (2.5 nM and 26 pM, respectively), as the 2.5 nM A6c134 affinity could be further improved by selecting variants in the α -chain. It is not yet clear whether monoclonal antibodies can be engineered further to have higher affinities and specificities for

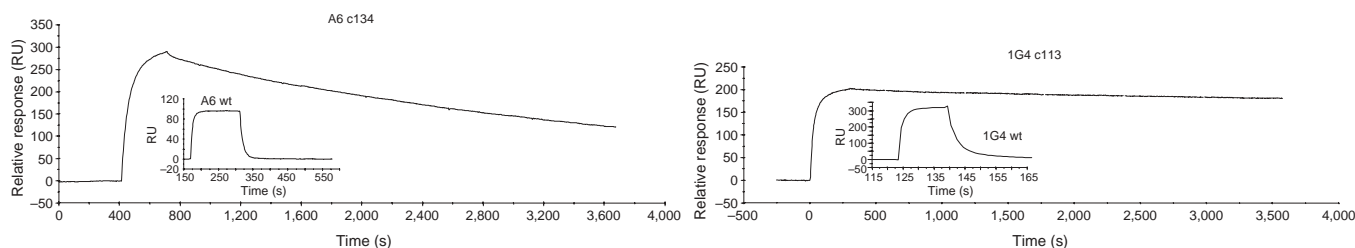


Figure 1 Biacore SPR binding of high-affinity TCRs compared to their parent wild-type TCRs. Left panel: A6c134 binding to HLA-A*0201-tax₁₁₋₁₉ ($K_d \approx 2.5$ nM, $t_{1/2} \approx 52$ min). Insert: wild-type A6 soluble TCR binding for comparison. Right panel: 1G4c113 binding to HLA-A*0201-NY-ESO-1₁₅₇₋₁₆₅ ($K_d \approx 20$ pM, $t_{1/2} \approx 1,000$ min). Insert: wild-type 1G4 soluble TCR binding for comparison.

peptide-HLAs, but it is likely that the structural framework of TCRs makes them intrinsically suitable for high-affinity binding of their natural peptide-HLA ligands. Indeed, preliminary X-ray structural analysis indicates that high-affinity TCRs bind peptide-HLA in a very similar mode to their respective wild-type parents (P.J. Rizkallah et al., unpublished data).

Our generation of high-affinity TCRs using relatively few mutations in the wild-type sequence proves that the architecture of the TCR-peptide-HLA interaction is amenable to high-affinity binding. Furthermore, many different binding loop sequences give rise to higher-affinity TCRs (see **Tables 2a,b**). It is likely that at least some of these mutations, or others having similar effects on TCR affinity, are generated by the natural recombination events occurring in developing T cells. However, all naturally occurring TCRs isolated to date have relatively low affinities falling within quite a narrow range (~ 1 – $100 \mu\text{M}$)¹. Therefore, these results seem to support the assertion that T cells expressing high-affinity TCRs must be eliminated by negative selection. However, considering the high peptide specificity of the high-affinity TCR mutants, it is difficult to believe that negative selection can occur only on the basis of interactions with self peptides. If this were the case, T cells with high-affinity TCRs, against, for example, viral peptides, should exist in the peripheral immune system. Rather, it seems likely that the T-cell repertoire that has passed through negative selection in the thymus can also be the subject of negative selection in the periphery²⁷ when encountering a ligand to which the TCR binds with a high affinity.

The low affinity of natural TCRs is one of the major hurdles for TCR-based therapeutic and diagnostic applications. These results demonstrate that the affinity of TCRs can be increased dramatically, by at least $\sim 10^6$ -fold, through directed evolution. The TCR phage display technology we have described here provides a generic approach for the affinity maturation of TCRs, as has been possible for antibodies for many years. Antibody phage display has also been used for the study of antibody-antigen interactions, structure-function relations and antibody folding and stability, and for the generation of novel human antibodies from naive libraries, thereby bypassing the immune system and its selection mechanisms. We expect that this technology will now enable all of these to be achieved in the future for the study and selection of TCRs.

METHODS

Design and construction of the vector for displaying A6 TCR on phage. To display TCR on phage, we designed a three-cistron phage display vector, pEX746, based on a pUC19 phagemid vector, pLitmus28 (NEB). Oligonucleotide primers were custom synthesized by MWG biotech. PAGE-purified library generation primers were custom synthesized by Sigma Genosys.

TCR α chains containing the mutation (TRAC threonine 48 \rightarrow cysteine¹⁵), and truncated immediately N-terminal of the natural membrane proximal cysteine, were expressed from a phagemid vector based upon pUC19. TCR β -chains, containing the mutation (TRBC serine 57 \rightarrow cysteine¹⁵), and similarly truncated, were expressed, in *cis*, under the control of the same *lacZ* promoter, as in-frame fusions to the geneIII coat protein of M13 bacteriophage.

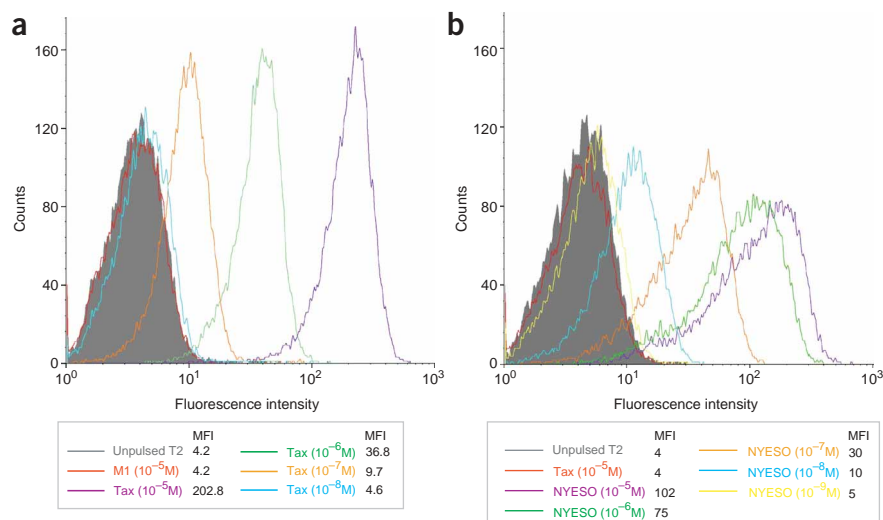


Figure 2 High-affinity TCR targeting of cell-surface pHLAs. HLA-A*0201⁺ T2 cells were pulsed, with either HTLV-1 tax_{11–19} (LLFGYPYVY), NY-ESO-1_{157–165} (SLLMWITQC), or influenza M1 peptide (GILGFVFTL), at the peptide concentration indicated, or were incubated without peptide (unpulsed). Mean fluorescence intensity (MFI) values are as indicated. The A6c134 tetramer-PE reagent can detect cells pulsed at 10 nM (10^{-8} M) peptide and shows no cross-reactivity to the endogenous peptides presented by unpulsed cells when compared to high level pulsing with null M1 peptide. The 1G4c113 tetramer-PE reagent is at least tenfold more sensitive, detecting 1 nM (10^{-9} M) peptide, and also shows no cross-reactivity to endogenous peptides.

The pelB leader gene and the second Shine-Dalgarno (SD) sequence were synthesized with primers YOL2 (5'-CAATCCAGCGGCTGCCGTAGGCAATAG GTATTTCATTATGACTGTCTCCTTGAAATAG-3'), YOL3 (5'-CTACGGCAG CCGCTGGATTGTTTACTCGCGGCCAGCCGCCATGGCCAG-3') and YOL4 (5'-GTTCTGTCTCCACTTCTCTGGCCATGGCCGGCTGGGCC G-3'). The TCR A6 α -chain was amplified from a plasmid containing the A6 α -chain gene with primers YOL5 (5'-CAGAAGGAAGTGGAGCAGAAC-3') and YOL6 (5'-CTTCTTAAAGAATTCTTAATTAACCTAGGTATTAGGAACCTT CTGGGCTGGGGAAG-3'). The third SD and M13 geneIII leader gene were synthesized with primers YOL7 (5'-GTTAATTAAGAATTCTTTAAGAAGGAG ATATACATATGAAAAAATTATTTCGCAATTC-3'), YOL8 (5'-CGCGCTG TGAGAAATAGAAAGGAACAACATAAGGAATTGCGAATAATAATTTTTCAT ATG-3') and YOL9 (5'-CTTCTATTCTCACAGCGCGCAGGCTGGTGTCACT CAGAC-3'). The TCR A6 β -chain was amplified from a plasmid containing the A6 β -chain gene with primers YOL9 and YOL10 (5'-ATGATGTCTAGATGCGG CCGCGTCTGTCTACCCAGGCCCTC-3'). M13 geneIII was amplified from M13 K07 with primers YOL11 (5'-GCATCTAGACATCATCACCATCATCACTA GACTGTTGAAAGTTGTTTAGCAAAAC-3') and YOL12 (5'-CTAGAGGGTAC CTTATTAAGACTCCTTATTACGCAGTATG-3'). SDII/pelB/ α /SDIII/ β gene was assembled with primers YOL1 (5'-TAATAATACGTATAATAATATTCTATTTC AAGGAGACAGTC-3') and YOL10 using overlapping PCR. GeneIII was first cloned into pLitmus28 at *XbaI/KpnI*, and then the assembled SDII/pelB/ α / SDIII/ β was cut with *SnaBI/XbaI* and cloned into the modified pLitmus28, containing geneIII.

After cloning, the constructs were screened by a phage ELISA. Clones which showed signal in the ELISA were sequenced with primers YOL 13 (5'-TCACAC AGGAAACAGCTATG-3'), YOL 17 (5'-ATTCGCAATTCCTTTAGTTG-3'), YOL 18 (5'-CAACTAAAGGAATTGCGAAT-3'), YOL19 (5'-ACCAGAGCAGTA CTTCGGGC-3') and YOL22 (5'-CATTTTCAGGGATAGCAAGC-3'). The final construct pEX746:A6 contains the α -chain of A6 TCR fused to the 3' end of the pelB leader, and the β -chain of the A6 TCR to the 3' of the M13 geneIII leader and 5' of the M13 geneIII.

Construction of CDR3 libraries. The central regions of A6 TCR CDR3s were targeted for introducing mutations. The mutations in A6 TCR CDR3 β were introduced by using PCR with the following forward primers: YOL59

Competition Biacore assays were done by incubating 1 nM 1G4c113 TCR with varying concentrations of soluble, nonbiotinylated A2-NY-ESO at room temperature (20–25 °C) for 30 min before binding measurement on a Biacore chip coated with 1,000 RU of A2-NY-ESO, as described previously¹⁸. The lowest concentration at which we could obtain reasonable SPR binding data was 1 nM TCR. We obtained k_{obs} values using BIAevaluation software and plotted them against HLA concentration (determined by OD₂₈₀ and an extinction coefficient calculated using Vector NTI software). Least squares fitting to the equation $k_{\text{obs}} = (k_{\text{obs}}^0/[\text{TCR}]) \times \{([\text{TCR}] - (1/2 \times ([\text{TCR}] + [\text{HLA}] + K_1)) + \sqrt{((1/2 \times ([\text{TCR}] + [\text{HLA}] + K_1))^2 - [\text{HLA}] \times [\text{TCR}])}\}$ was performed using Origin 6.0 software (Microcal).

TCR tetramerization and cell staining. TCRs were tetramerized by engineering a C-terminal biotinylation tag onto the β -chain and tetramerizing with fluorescently labeled streptavidin²¹. HLA-A*0201⁺ T2 cells were pulsed, with either HTLV-1 tax_{11–19} (LLFGYPVYV), NY-ESO-1_{157–165} (SLLMWITQC), or influenza M1 peptide (GILGFVFTL), at the peptide concentration indicated, or were incubated without peptide (unpulsed), for 90 minutes at 37 °C. After a wash step in PBS, cells were incubated with A6c134 tetramer-PE (10 $\mu\text{g}/\text{ml}$), or 1G4c113 tetramer-PE (10 $\mu\text{g}/\text{ml}$), for 10 min at room temperature (20–25 °C). After incubation, cells were washed and TCR tetramer-PE binding was examined by flow cytometry using a FACS Vantage SE (BD Biosciences) and data were analyzed using CellQuest software (BD Biosciences).

Note: Supplementary information is available on the Nature Biotechnology website.

ACKNOWLEDGMENTS

We would like to thank the following for supplying plasmids containing wild-type TCR genes: W.E. Biddison for A6, V. Cerundolo for 1G4 and MM15, E. Gostick for ILAK, S. Burrows for LC13, G.F. Gao for JM22, H. Gaston for AH1.23, S. Gadola for CD1d and Paul Bowness for GRB. We would like to thank M. Sami, P. Todorov and A. Johnson for assistance with protein purification, Martin Green, R. Ashfield and N. Lissin for helpful discussions and critical reading of the manuscript, B. Laugel and A.K. Sewell for additionally sharing data before publication and D. Sutton for assistance in preparing figures.

COMPETING INTERESTS STATEMENT

The authors declare competing financial interests (see the Nature Biotechnology website for details).

Received 3 August; accepted 16 December 2004

Published online at <http://www.nature.com/naturebiotechnology/>

1. van der Merwe, P.A. & Davis, S.J. Molecular interactions mediating T cell antigen recognition. *Annu. Rev. Immunol.* **21**, 659–684 (2003).
2. Boulter, J.M. *et al.* Stable, soluble T-cell receptor molecules for crystallization and therapeutics. *Protein Eng.* **16**, 707–711 (2003).
3. Garboczi, D.N. *et al.* Structure of the complex between human T-cell receptor, viral peptide and HLA-A2. *Nature* **384**, 134–141 (1996).
4. Jager, E. *et al.* Simultaneous humoral and cellular immune response against cancer-testis antigen NY-ESO-1: definition of human histocompatibility leukocyte antigen (HLA)-A2-binding peptide epitopes. *J. Exp. Med.* **187**, 265–270 (1998).

5. Kohler, G. & Milstein, C. Continuous cultures of fused cells secreting antibody of predefined specificity. *Nature* **256**, 495–497 (1975).
6. Clackson, T., Hoogenboom, H.R., Griffiths, A.D. & Winter, G. Making antibody fragments using phage display libraries. *Nature* **352**, 624–628 (1991).
7. Hanes, J., Schaffitzel, C., Knappik, A. & Pluckthun, A. Picomolar affinity antibodies from a fully synthetic naive library selected and evolved by ribosome display. *Nat. Biotechnol.* **18**, 1287–1292 (2000).
8. Smith, I.E. New drugs for breast cancer. *Lancet* **360**, 790–792 (2002).
9. Shusta, E.V., Holler, P.D., Kieke, M.C., Kranz, D.M. & Wittrup, K.D. Directed evolution of a stable scaffold for T-cell receptor engineering. *Nat. Biotechnol.* **18**, 754–759 (2000).
10. Holler, P.D. *et al.* In vitro evolution of a T cell receptor with high affinity for peptide/MHC. *Proc. Natl. Acad. Sci. USA* **97**, 5387–5392 (2000).
11. Holler, P.D., Lim, A.R., Cho, B.K., Rund, L.A. & Kranz, D.M. CD8(-) T cell transfectants that express a high affinity T cell receptor exhibit enhanced peptide-dependent activation. *J. Exp. Med.* **194**, 1043–1052 (2001).
12. Holler, P.D. & Kranz, D.M. Quantitative analysis of the contribution of TCR/peptide/MHC affinity and CD8 to T cell activation. *Immunity* **18**, 255–264 (2003).
13. Holler, P.D., Chlewicki, L.K. & Kranz, D.M. TCRs with high affinity for foreign pMHC show self-reactivity. *Nat. Immunol.* **4**, 55–62 (2003).
14. Weidanz, J.A., Card, K.F., Edwards, A., Perlstein, E. & Wong, H.C. Display of functional alphabeta single-chain T-cell receptor molecules on the surface of bacteriophage. *J. Immunol. Methods* **221**, 59–76 (1998).
15. Lefranc, M.-P.L.G. *The T Cell Receptor Facts Book* (Academic Press, London, 2001).
16. Garboczi, D.N. *et al.* Assembly, specific binding, and crystallization of a human TCR-alphabeta with an antigenic Tax peptide from human T lymphotropic virus type 1 and the class I MHC molecule HLA-A2. *J. Immunol.* **157**, 5403–5410 (1996).
17. Khalifa, M.B., Choulier, L., Lortat-Jacob, H., Altschuh, D. & Vernet, T. BIACORE data processing: an evaluation of the global fitting procedure. *Anal. Biochem.* **293**, 194–203 (2001).
18. Karlsson, R. Real-time competitive kinetic analysis of interactions between low-molecular-weight ligands in solution and surface-immobilized receptors. *Anal. Biochem.* **221**, 142–151 (1994).
19. Hutchinson, S.L. *et al.* The CD8 T cell coreceptor exhibits disproportionate biological activity at extremely low binding affinities. *J. Biol. Chem.* **278**, 24285–24293 (2003).
20. Altman, J.D. *et al.* Phenotypic analysis of antigen-specific T lymphocytes. *Science* **274**, 94–96 (1996).
21. Laugel, B. *et al.* Design of soluble recombinant T cell receptors for antigen targeting and T cell inhibition. *J. Biol. Chem.* **280**, 1882–1892 (2004).
22. Schirle, M. *et al.* Identification of tumor-associated MHC class I ligands by a novel T cell-independent approach. *Eur. J. Immunol.* **30**, 2216–2225 (2000).
23. Cohen, C.J., Denkberg, G., Lev, A., Epel, M. & Reiter, Y. Recombinant antibodies with MHC-restricted, peptide-specific, T-cell receptor-like specificity: new tools to study antigen presentation and TCR-peptide-MHC interactions. *J. Mol. Recognit.* **16**, 324–332 (2003).
24. Cohen, C.J. *et al.* Direct phenotypic analysis of human MHC class I antigen presentation: visualization, quantitation, and *in situ* detection of human viral epitopes using peptide-specific, MHC-restricted human recombinant antibodies. *J. Immunol.* **170**, 4349–4361 (2003).
25. Biddison, W.E. *et al.* Tax and M1 peptide/HLA-A2-specific Fabs and T cell receptors recognize nonidentical structural features on peptide/HLA-A2 complexes. *J. Immunol.* **171**, 3064–3074 (2003).
26. Held, G. *et al.* Dissecting cytotoxic T cell responses towards the NY-ESO-1 protein by peptide/MHC-specific antibody fragments. *Eur. J. Immunol.* **34**, 2919 (2004).
27. Anderton, S.M., Radu, C.G., Lowrey, P.A., Ward, E.S. & Wraith, D.C. Negative selection during the peripheral immune response to antigen. *J. Exp. Med.* **193**, 1–11 (2001).
28. Garboczi, D.N., Hung, D.T. & Wiley, D.C. HLA-A2-peptide complexes: refolding and crystallization of molecules expressed in *Escherichia coli* and complexed with single antigenic peptides. *Proc. Natl. Acad. Sci. USA* **89**, 3429–3433 (1992).